Deep-Sea Research II ∎ (∎∎∎∎) ∎∎∎–∎∎∎

Contents lists available at ScienceDirect

Deep-Sea Research II

journal homepage: www.elsevier.com/locate/dsr2

Regular article

Dissolved and particulate phosphorus distributions and elemental stoichiometry throughout the Chukchi Sea

Meryssa M. Piper [a], Claudia R. Benitez-Nelson [a,*], Karen E. Frey [b], Matthew M. Mills [c], Sharmila Pal [a]

[a] Department of Earth and Ocean Sciences & Marine Science Program, University of South Carolina, Columbia, SC, USA
[b] Graduate School of Geography, Clark University, Worcester, MA, USA
[c] Department of Earth System Science, Stanford, CA, USA

ARTICLE INFO

Keywords:
USA
Alaska
Chukchi Sea
Polar region
Phosphorus
Water column
Sea ice

ABSTRACT

As a major gateway from the Pacific to the open Arctic Ocean, biogeochemical transformations of nutrients in the Chukchi Sea are important for understanding the Arctic ecosystem as a whole. This study examines the biogeochemical cycling of the macronutrient phosphorus (P) relative to carbon (C) and nitrogen (N) in the eastern Chukchi Sea during the ICESCAPE mission. Sea ice and water column dissolved and particulate P samples were collected during summer expeditions in 2010 ($n=543$) and 2011 ($n=553$). Nearly all forms of P were higher in Pacific Winter Waters (PWW), indicating the potential importance of PWW to Chukchi Sea nutrient pools. Annual means of P concentrations in all its forms in the offshore waters throughout the Chukchi Sea were also consistently higher ($TP_{2010}=1.56\pm0.61$ μM, $TP_{2011}=1.67\pm0.68$ μM) relative to waters inshore and within the Alaska Coastal Current (ACC), suggesting coastal inputs were relatively minor during our sampling. Rather, biological modification of P pools dominated, with 30–40% of the total dissolved P pool (TDP) and nearly 50% of the total particulate P pool (TPP) comprised of organic P. Nutrient analyses of first year sea ice suggest that sea ice melt contains highly variable P concentrations that span an order of magnitude depending on particulate matter content. As such, sea ice melt may contribute significant nutrients to summer waters on a transient basis. Low N:P ratios (<2) within the mixed layer are consistent with summertime N limitation of biological production and demonstrate that the Chukchi Sea is a major source of excess P to other regions of the Arctic Ocean. Deeper water column dissolved N:P ratios of 7–9.1, while lower than the canonical Redfield ratio, are consistent with particulate N:P ratios of a diatom-dominated biological community. Combined, results suggest that the eastern Chukchi Sea plays an important role in the composition and magnitude of P that ultimately reaches other Arctic Ocean waters.

1. Introduction

The Arctic Ocean is undergoing significant changes in its physical and biogeochemical environment due to rising water temperatures, melting sea ice, and increases in riverine discharge (Arnell, 2005, Serreze et al., 2007; Stroeve et al., 2012; Post et al., 2013). The 2007–2010 average September sea ice extent declined by 40% compared to measurements taken 20–30 years earlier, with sea ice distributions reaching record lows in 2012 (Stroeve et al., 2012). Furthermore, models suggest that the entire Arctic will become seasonally ice free as early as 2040 (Holland et al., 2006; Wang and Overland, 2009). Indeed, some Arctic seas have already begun to experience ice-free seasons, including the Chukchi Sea (Stroeve et al., 2012).

As nutrient-rich Pacific waters make their way further into the Arctic Ocean through the Chukchi Sea via the Bering Strait, they are impacted by a variety of processes, including coastal inputs, sediment resuspension, redox reactions (e.g., denitrification), variable ice cover, and primary production (Frey et al., 2014). Similar to the rest of the Arctic Ocean, the Chukchi Sea has experienced an increase in satellite derived net primary production of almost 50% over the past 12 years, among the highest increases in primary production throughout the region (Arrigo and van Dijken, 2015). This dramatic increase is likely due to greater light penetration as a result of declining sea ice and an enhanced number of melt ponds (Arrigo and van Dijken, 2011, 2015, Lowry et al., 2015; Grebmeier, 2012; Petrenko et al., 2013). It is important to note that the increase in water column primary productivity does not consider possible alterations in sea ice primary production, which contributes significantly to primary production within the central Arctic Ocean (Gosselin et al., 1997); nor does this estimate take into account the

* Corresponding author. Tel.: +1 803 777 0018
E-mail address: cbnelson@geol.sc.edu (C.R. Benitez-Nelson).

http://dx.doi.org/10.1016/j.dsr2.2016.05.009
0967-0645/

changes in primary productivity occurring beneath sea ice, such as the massive under ice bloom observed in 2011 (Arrigo et al., 2012). It is hypothesized that up to 70% of the resulting carbon fixed in the southeast Chukchi from water column primary production may settle to the sea floor where it can be utilized by benthic fauna (Cooney and Coyle, 1982; Walsh et al., 1989; McTigue et al., 2015).

During the summer months, waters make their way through the eastern Chukchi Sea in one of two major water masses: the Alaskan Coastal Waters or the Chukchi Summer Waters (von Appen and Pickart 2012; Brugler et al., 2014); the latter is also referred to as Bering Sea Water (Gong and Pickart, 2015), Summer Bering Sea Water (Steele et al., 2004), and Eastern Chukchi Summer Water (Shimada et al., 2001). The Alaskan Coastal Waters are pumped through the Chukchi Sea by the Alaskan Coastal Current (ACC) and remain trapped within 50 km of the coast (Schumacher and Reed, 1986). However, the Chukchi Summer Waters (CSW) move through the Chukchi Sea in a variety of pathways. As they make their way through the Chukchi Sea, these new summer waters mingle and aid in the transportation of remaining Pacific Winter Water (PWW). The PWW is hypothesized to form during sea ice formation, increasing water density and concentrating nutrients (Lowry et al., 2015). Both summer waters and remnant winter waters traverse the Chukchi Sea via four main routes: Long Strait, Herald Valley, Central Channel, and Barrow Canyon. Barrow Canyon has the fastest flowing output with rates up to 1 Sv during the summer months, and is the major exit pathway assessed in this study (Münchow et al., 1999; Weingartner et al., 2005). As waters exit Barrow Canyon, they are focused into the Beaufort Shelf Jet, a narrow shelf break jet, as they make their way into the Beaufort Sea (Pickart, 2004; Nikolopoulos et al., 2009).

Phosphorus (P) is an essential macronutrient that influences biological production and plankton community structure in a variety of marine systems (Karl, 2014). Within the ocean, P occurs in both organic and inorganic forms and is actively partitioned between dissolved and particulate phases via a suite of biologically and chemically mediated reactions. While many previous studies have focused mainly on inorganic P, as it is the most readily available form (e.g., Benitez-Nelson, 2000, Paytan and McLaughlin, 2007), numerous studies now recognize that organisms also utilize organic P compounds even when inorganic P concentrations are relatively high (>0.2 μM) (e.g., Mortazavil et al., 2000; Dyhrman et al., 2006; Sylvan et al., 2006; Huang and Zhang, 2010; Karl, 2014). Therefore, understanding the distribution and concentrations of all P forms is critical for examining nutrient dynamics. Nevertheless, relatively little is known regarding the distribution of P within marine dissolved and particulate matter in the Arctic Ocean, particularly in the Chukchi Sea.

In this study, we analyzed multiple water column and sea ice core samples for dissolved and particulate P that were collected throughout the eastern Chukchi Sea during the summers of 2010 and 2011 as part of NASA's Impact of Climate Change on the Ecosystems and Chemistry of the Arctic Pacific Environment (ICESCAPE) mission. In order to fully understand the processes influencing P biogeochemistry, total phosphorus (TP) was further broken down into total dissolved P (TDP) and total particulate P (TPP). These pools were then chemically separated into inorganic and organic phases: particulate inorganic P (PIP), particulate organic P (POP), soluble reactive P (SRP), and dissolved organic P (DOP). The goal of this study was to improve our understanding of the source, composition, and distribution of dissolved and particulate P within this climate impacted ecosystem.

2. Materials and methods

2.1. Study site and sample collection

As part of the ICESCAPE field mission, the Chukchi Sea was sampled during two summer cruises, 15 June–22 July, 2010 and 25 June–29 July, 2011, aboard the USCGC *Healy* (WAGB-20) (Fig. 1). During the 2010 cruise, water column ($n=135$) and ice ($n=10$) stations were sampled from the Bering Strait northward to Barrow Canyon. Dissolved and/or particulate P were sampled from 121 of these stations with a total of 543 samples analyzed in 2010. Due to decreased ice cover, the 2011 cruise extended from the Bering Strait northward to the southern Beaufort Sea; 173 stations were sampled, including nine ice stations. Dissolved and particulate data were analyzed in 553 samples from 104 stations. All ice stations were comprised of only first year ice.

Both cruises sampled multiple water masses. The ACC was identified by high temperatures (≥ 3 °C) and salinities ≥ 30, while the CSW were characterized by lower temperatures (-1 to 2 °C), and similar salinities (Brugler et al., 2014). Atlantic deep waters were characterized by low temperatures (<-1.26 °C) and high salinities (>33.64) (Brugler et al., 2014). Lastly, some stations were able to capture remaining PWW. These waters were characterized by temperatures lower than -1.6 °C and salinities higher than 31.5, consistent with other work from the ICESCAPE mission (Brown et al., 2015, Gong and Pickart, 2015, Lowry et al., 2015, Mills et al., 2015).

Water column data were obtained by deploying a conductivity, temperature, and depth sensor (CTD) on a rosette system equipped with twelve 30 L Niskin bottles. The CTD/rosette system also included a photosynthetically available radiation (PAR) sensor and fluorometer. Water samples were collected at standard depths (roughly 2, 10, 25, 50, 100, 200, 500, 1000, and 2000 m depending on water depth) and analyzed for chlorophyll *a* and dissolved inorganic nutrients (i.e., nitrate silicate, and phosphate), as described in Brown et al. (2015) and Mills et al. (2015) (all nutrient data available at seabass.gsfc.nasa.gov).

Ice core data were collected using a custom built CRREL ice coring system with a diameter of 10 cm. Cores used for nutrient analysis during the 2010 cruise ($n=21$) were melted in a known amount of filtered surface seawater (usually 2 L per 10 cm section), with salinity measurements recorded pre and post melt. As such, dissolved nutrient data are not available from ice cores sampled for particulate nutrients in 2010. Samples were then filtered for particulate P analysis onto a 1 N HCl washed and 500 °C combusted, 25 mm GF/F (~0.7 μm) and frozen until analysis. In 2011, the ice cores used for nutrient measurements were melted without dilution. Particulate and dissolved nutrient analyses were conducted on the resulting melt water. During the 2010 cruise, ice cores were both visibly sediment laden and sediment free, while in 2011, all ice core samples were visibly sediment free.

2.2. Ship board analyses

Continuous profiles of chlorophyll *a* fluorescence were collected at each station using a Wetlabs fluorometer. Additional samples for chlorophyll *a* analysis were filtered onto a 25 mm GF/F (~0.7 μm), placed in 5 mL of 90% acetone and extracted in the dark at 3 °C for 24 h. Chlorophyll *a* concentrations were then measured fluorometrically using a Turner fluorometer 10-AU (Holm-Hansen et al., 1965). A chlorophyll *a* standard (Sigma-Aldrich #C5753) was used to calibrate fluorescence-based chlorophyll *a* measurements in remaining samples (Holmes et al., 2000).

Total inorganic nutrients (unfiltered) were analyzed on a segmented continuous flow auto analyzer within a few hours of

Please cite this article as: Piper, M.M., et al., Dissolved and particulate phosphorus distributions and elemental stoichiometry throughout the Chukchi Sea. Deep-Sea Res. II (2016), http://dx.doi.org/10.1016/j.dsr2.2016.05.009

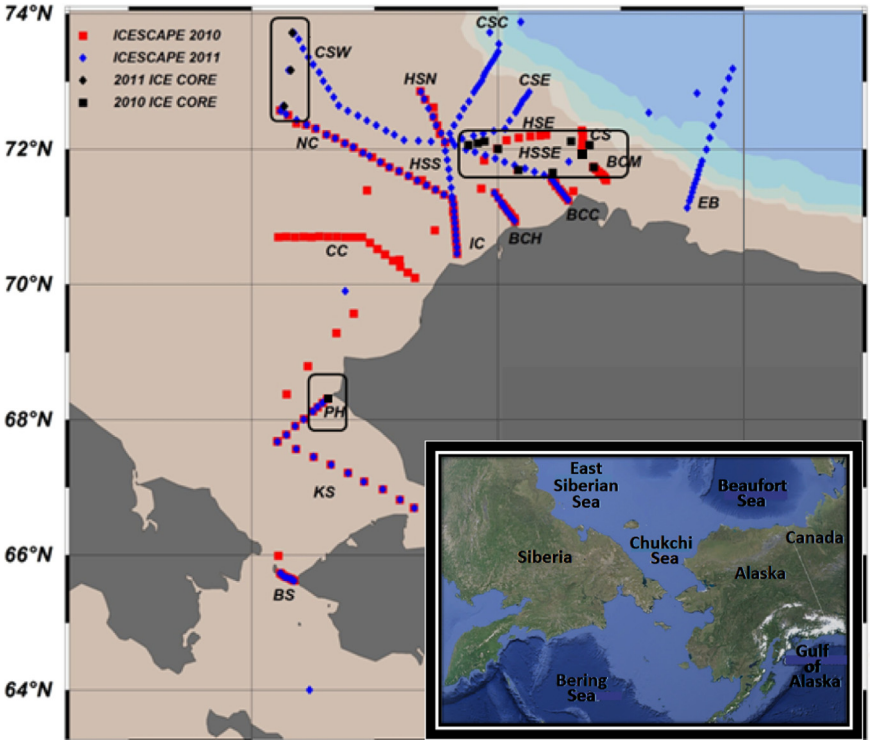

Fig. 1. Map of cruise track for 2010 (squares) and 2011 (diamonds); ice stations further emphasized with black rectangles. Sections of the cruise were grouped and labeled for comparison; Bering Strait (BS), Kotzebue Sound (KS), Point Hope (PH), Center Channel (CC), Icy Cape (IC), North Chukchi (NC), Hanna Shoal South (HSS), Chukchi Slope West (CSW), Hanna Shoal North (HSN), Barrow Canyon Head (BCH) Barrow Canyon Center (BCC) Hanna Shoal South East (HSSE), Hanna Shoal East (HSE), Chukchi Slope East (CSE), Chukchi Slope Center (CSC), Barrow Canyon Mouth (BCM), Chukchi Slope (CS), and East of Barrow (EB). (For interpretation of the references to color in this figure legend, the reader is referred to the web version of this article.)

collection. [NO_3^-], [NO_2^-] and [$Si(OH_4)$] analyses were performed using a modification of the method outlined by Armstrong et al. (1967). [NH_4^+] was determined fluorometrically according to Kérouel and Aminot (1997) and [$H_2PO_4^-$] was measured using the ammonium molybdate method described in Bernhardt and Wilhelms (1967).

2.3. Dissolved P speciation

Dissolved P samples were collected by filtering ~40 mL of seawater through a 500 °C pre-combusted and 1 N HCl washed, 25 mm GF/F (~0.7 μm) and frozen until analysis. Phosphate or soluble reactive P (SRP) was measured according to the spectrophotometric method described in Koroleff (1983). Total dissolved P (TDP) was measured using the high temperature ash/hydrolysis technique outlined in Monaghan and Ruttenberg (1999). Both SRP and TDP analyses have a detection limit of 0.07 μM; dissolved organic P (DOP) is defined as the difference between TDP and SRP. Approximately 11% of samples were run in duplicate, with an average coefficient of variation (CV) of 6.0%. It is important to note that SRP and DOP are analytically defined; therefore, SRP may contain acid-labile organic compounds, such as simple sugars, while DOP may contain acid insoluble inorganic compounds, such as polyphosphate (Monaghan and Ruttenberg, 1999, Benitez-Nelson, 2000).

2.4. Particulate analyses

Samples for particulate nitrogen (PN) and particulate organic carbon (POC) were filtered onto a pre-combusted 25 mm GF/F (~0.7 μm) and stored frozen until analysis. Particulate P samples were filtered onto a 500 °C pre-combusted, 1 N HCl washed, 25 mm Whatman GF/F (~0.7 μm), frozen and stored until analysis. Ice core particulate P filters were split for total particulate carbon (PC) and PN analyses. The POC filters were fumed in a dessicator with concentrated HCl overnight. The PN, PC and POC samples were subsequently dried at 60 °C, and packed into tin capsules for elemental analysis. Peach leaves and glutamic acid were used as calibration standards (Mills et al., 2015).

Total particulate phosphorus (TPP) and particulate inorganic phosphorus (PIP) were analyzed according to the ash/hydrolysis method outlined by Aspila et al. (1976) as modified by Benitez-Nelson et al. (2007). Particulate organic phosphorus (POP) was determined by the difference, i.e. TPP − PIP = POP. Accuracy and reproducibility for each sample set was assessed from quadruplicate analysis of two certified reference materials (NIST 1515, tomato leaves, certified 0.216% P by weight, and NIST 1673a, estuarine sediment, certified 0.027% P by weight). The distinction between PIP and POP concentrations is again operationally defined. Therefore it is possible that the inorganic P fraction contains some labile organic P compounds and vice versa (Benitez-Nelson et al., 2004). Approximately, 5% of the samples were run in duplicate, with an average CV of 5.3%. Reference materials were always within 5% of expected values. Filter blanks were always below the 0.07 μM P limit of detection.

2.5. Statistics

All data sets were tested for normality using the Lillifor's significance correction K–S test (Lilliefors, 1967). Much of the data exhibits small departures from normality. Due to their robust nature, parametric t-tests were used to determine differences at the $\alpha = 0.05$ significance level. One standard deviation is presented alongside all arithmetic means and as error bars. When summed data are presented instead of means, total errors are propagated using the analytical uncertainties of each measurement.

Please cite this article as: Piper, M.M., et al., Dissolved and particulate phosphorus distributions and elemental stoichiometry throughout the Chukchi Sea. Deep-Sea Res. II (2016), http://dx.doi.org/10.1016/j.dsr2.2016.05.009

Table 1
2010 P (M) and N (M) pool averages throughout the eastern Chukchi Sea. Significant differences ($p < 0.05$) noted via the following symbols: annual *, inshore (a) – offshore (b) – ACC (c), winter water – non-winter water (+), mixed (a) – mid (b) – Bottom (c).

2010	TP (μM)	TDP (μM)	SRP (μM)	DOP (μM)	DIN (μM)	TPP (μM)	PIP (μM)	POP (μM)	POC (μM)	PN (μM)
Chukchi Sea	1.56 ± 0.61*, $n=250$	1.26 ± 0.53*, $n=308$	0.74 ± 0.43*, $n=307$	0.52 ± 0.36, $n=307$	3.74 ± 4.87*, $n=417$	0.22 ± 0.24*, $n=407$	0.11 ± 0.14*, $n=406$	0.09 ± 0.14*, $n=405$	30.12 ± 33.01*, $n=378$	3.70 ± 3.36* , $n=372$
Mixed	$^{c}1.43 \pm 0.56$*, $n=91$	$^{bc}1.11 \pm 0.48$, $n=117$	$^{bc}0.59 \pm 0.33$, $n=116$	$^{0.51} \pm 0.32$, $n=116$	$^{bc}0.75 \pm 1.95$*, $n=146$	0.21 ± 0.23*, $n=144$	0.11 ± 0.14*, $n=144$	0.08 ± 0.14*, $n=144$	33.49 ± 38.96*, $n=119$	3.74 ± 3.37*, $n=119$
Mid	$^{c}1.58 \pm 0.64$*, $n=134$	$^{ac}1.30 \pm 0.53$*, $n=161$	$^{ac}0.77 \pm 0.42$*, $n=161$	0.52 ± 0.39, $n=161$	$^{ac}4.94 \pm 5.08$*, $n=234$	0.22 ± 0.26*, $n=228$	0.11 ± 0.15*, $n=227$	0.09 ± 0.15*, $n=227$	28.64 ± 30.82*, $n=225$	3.64 ± 3.44*, $n=221$
Bottom	$^{ab}1.90 \pm 0.49$, $n=25$	$^{ab}1.68 \pm 0.48$, $n=30$	$^{ab}1.14 \pm 0.50$, $n=30$	0.54 ± 0.39, $n=30$	$^{ab}7.93 \pm 5.23$*, n=37	0.23 ± 0.18, $n=35$	0.13 ± 0.14, $n=35$	0.08 ± 0.10, $n=34$	28.06 ± 22.71*, $n=34$	3.97 ± 2.72*, $n=32$
Non-PWW	$^{+}1.65 \pm 0.73$, $n=36$	$^{+}1.19 \pm 0.57$, $n=45$	$^{+}0.70 \pm 0.42$, $n=45$	0.50 ± 0.40, $n=45$	$^{+}2.06 \pm 3.51$, $n=114$	0.33 ± 0.32*, $n=59$	0.14 ± 0.16*, $n=39$	$^{+}0.17 \pm 0.21$*, $n=41$	$^{+}40.69 \pm 45.37$*, $n=106$	4.44 ± 3.60*, $n=104$
PWW	$^{+}2.21 \pm 0.50$*, $n=23$	$^{+}1.90 \pm 0.44$*, $n=28$	$^{+}1.44 \pm 0.43$ $n=28$	0.46 ± 0.30, $n=26$	$^{+}12.62 \pm 3.31$, $n=44$	0.25 ± 0.18, $n=38$	0.13 ± 0.14, $n=27$	$^{+}0.10 \pm 0.10$, $n=26$	$^{+}30.06 \pm 24.90$, $n=42$	3.85 ± 3.22*, $n=40$
Inshore	1.46 ± 0.52*, $n=21$	1.26 ± 0.50*, $n=22$	$^{b}0.57 \pm 0.19$, $n=22$	$^{b}0.69 \pm 0.38$*, $n=22$	$^{b}2.12 \pm 2.88$*, $n=32$	0.18 ± 0.16*, $n=32$	$^{b}0.07 \pm 0.10$, $n=32$	$^{c}0.08 \pm 0.11$*, n=32	24.93 ± 24.13* $n=30$	$^{b}3.00 \pm 1.74$*, $n=30$
ACC	^{b} 1.28 ± 0.43, $n=39$	^{b} 1.10 ± 0.42, $n=43$	$^{b}0.50 \pm 0.17$, $n=43$	0.57 ± 0.35, $n=43$	$^{b}1.24 \pm 2.33$, $n=54$	$^{0.15} \pm 0.09$, $n=57$	$^{b}0.08 \pm 0.07$, $n=57$	$^{ab}0.03 \pm 0.05$, $n=57$	^{b} 17.65 ± 8.48*, $n=55$	$^{b}2.38 \pm 1.34$, $n=55$
Offshore	$^{c}1.63 \pm 0.63$*, $n=190$	$^{c}1.29 \pm 0.55$*, $n=243$	$^{ac}0.80 \pm 0.46$*, n=242	$^{a}0.49 \pm 0.36$, $n=242$	$^{ac}4.30 \pm 5.16$*, $n=331$	$^{c}0.23 \pm 0.26$*, $n=318$	$^{ac}0.12 \pm 0.16$*, $n=317$	$^{c}0.10 \pm 0.15$*, $n=316$	$^{c}32.97 \pm 36.01$*, $n=293$	$^{ac}4.03 \pm 3.67$*, $n=287$

Table 2
2011 P (M) and N (M) pool averages throughout the eastern Chukchi Sea. Significant differences noted via the following symbols: annual *, inshore (a) – offshore (b) – ACC (c), winter water – non-winter water (+), mixed (a) – mid (b) – Bottom (c).

2011	TP (μM)	TDP (μM)	SRP (μM)	DOP (μM)	DIN (μM)	TPP (μM)	PIP (μM)	POP (μM)	POC (μM)	PN (μM)
Chukchi Sea	1.67 ± 0.68*, $n=351$	1.37 ± 0.57*, $n=519$	0.89 ± 0.48*, $n=500$	0.49 ± 0.30, $n=500$	5.61 ± 6.80*, $n=518$	0.16 ± 0.18*, $n=515$	0.08 ± 0.11*, $n=515$	0.06 ± 0.11*, $n=514$	13.92 ± 14.81*, $n=471$	2.22 ± 2.25*, $n=458$
Mixed	$^{bc}1.25 \pm 0.36$*, $n=132$	$^{bc}1.03 \pm 0.29$, $n=163$	$^{bc}0.58 \pm 0.21$, $n=156$	$^{c}0.45 \pm 0.23$, $n=156$	$^{bc}0.43 \pm 1.08$*, $n=163$	$^{c}0.15 \pm 0.14$*, $n=163$	$^{c}0.08 \pm 0.08$*, $n=163$	0.05 ± 0.09*, $n=163$	$^{c}13.43 \pm 14.56$*, $n=157$	$^{c}2.02 \pm 1.92$*, $n=157$
Mid	$^{a}1.91 \pm 0.70$*, $n=134$	$^{a}1.51 \pm 0.59$*, $n=293$	$^{a}1.03 \pm 0.50$*. $n=285$	$^{b}0.49 \pm 0.30$, $n=285$	$^{ac}7.56 \pm 6.97$*, $n=292$	$^{b}0.14 \pm 0.19$*, $n=289$	$^{b}0.07 \pm 0.11$*, $n=289$	0.05 ± 0.11*, $n=288$	$^{b}13.35 \pm 15.67$*, $n=256$	2.23 ± 2.53*, $n=243$
Bottom	$^{a}1.96 \pm 0.70$, $n=56$	$^{a}1.64 \pm 0.60$, $n=63$	$^{a}1.07 \pm 0.49$, $n=59$	$^{ab}0.61 \pm 0.41$, $n=59$	$^{ab}9.91 \pm 6.97$*, $n=63$	$^{ab}0.25 \pm 0.22$, $n=63$	$^{ab}0.14 \pm 0.13$, $n=63$	$^{a}0.09 \pm 0.15$, $n=63$	$^{ab}17.78 \pm 10.64$*, $n=58$	$^{a}2.74 \pm 1.75$*, $n=58$
Non-PWW	$^{+}1.43 \pm 0.51$, $n=99$	$^{+}1.22 \pm 0.39$, $n=120$	$^{+}0.69 \pm 0.29$, $n=120$	0.53 ± 0.25, n=120	$^{+}1.13 \pm 2.90$, $n=121$	$^{+}0.17 \pm 0.19$*, $n=99$	$^{+}0.08 \pm 0.12$*, $n=68$	$^{+}0.06 \pm 0.12$*, $n=44$	$^{+}15.89 \pm 16.70$*, $n=111$	$^{+}2.17 \pm 1.97$*, $n=110$
PWW	$^{+}2.46 \pm 0.55$*, $n=62$	$^{+}2.15 \pm 0.54$*, $n=65$	$^{+}1.56 \pm 0.45$, $n=65$	0.58 ± 0.34, $n=65$	$^{+}13.66 \pm 6.21$, $n=65$	$^{+}0.30 \pm 0.19$, $n=62$	$^{+}0.11 \pm 0.11$, $n=56$	$^{+}0.17 \pm 0.09$, $n=44$	$^{+}28.37 \pm 20.20$, $n=63$	$^{+}4.66 \pm 2.98$*, $n=62$
Inshore	$^{bc}1.12 \pm 0.16$*, $n=22$	$^{bc}1.00 \pm 0.15$*, $n=24$	$^{bc}0.49 \pm 0.13$, $n=21$	0.53 ± 0.18, $n=21$	$^{bc}0.22 \pm 0.18$*, $n=24$	$^{b}0.11 \pm 0.06$*, $n=24$	$^{bc}0.05 \pm 0.05$, $n=24$	$^{b}0.02 \pm 0.04$*, $n=24$	$^{bc}10.12 \pm 2.97$*, $n=24$	$^{bc}1.55 \pm 0.66$*, $n=23$
ACC	$^{ab}1.31 \pm 0.32$, $n=38$	$^{ab}1.12 \pm 0.30$, $n=43$	$^{ab}0.58 \pm 0.19$, $n=35$	0.57 ± 0.29, $n=35$	$^{ab}1.45 \pm 1.78$, $n=43$	0.15 ± 0.08, $n=43$	$^{a}0.08 \pm 0.07$, $n=43$	$^{b}0.03 \pm 0.05$, $n=43$	$^{a}12.38 \pm 5.64$*, $n=43$	$^{a}2.04 \pm 1.02$, $n=43$
Offshore	$^{ac}1.76 \pm 0.70$*, $n=291$	$^{ac}1.41 \pm 0.59$*, $n=452$	$^{ac}0.94 \pm 0.49$*, $n=444$	0.48 ± 0.30, $n=444$	$^{ac}6.29 \pm 7.01$*, $n=451$	$^{a}0.16 \pm 0.19$*, $n=448$	$^{a}0.08 \pm 0.11$*, $n=448$	$^{ac}0.06 \pm 0.11$*, $n=447$	$^{a}14.31 \pm 15.84$*, $n=404$	$^{a}2.28 \pm 2.40$*, $n=392$

3. Results

3.1. Physical regime

Between the 2010 and 2011 cruises, important differences in the physical regime of the water column were observed. During the 2011 cruise, greater sea ice retreat allowed samples to be collected farther into the Chukchi and the Beaufort seas. Gong and Pickart (2015) noted that the winds during 2010 were weaker and more variable from July to September than the climatological mean, while the 2011 northeasterly winds were more prominent and lasted from June to October. These winds likely contributed to the observed decrease in ACC strength, and a reduction in the Beaufort Shelf Jet during 2011 compared to 2010.

In order to better understand spatial and temporal differences within the eastern Chukchi Sea, P data were sorted by year, depth (mixed layer, mid waters, and bottom waters), water mass (winter water and non-winter water), and region (inshore of ACC, referred to as inshore, the ACC, and offshore of ACC waters, referred to as offshore). Mixed layer depths were determined using a change in density from surface values of greater than 0.125 g cm^{-3}, consistent with temperature differences of 0.5 °C, as outlined by Monterey and Levitus (1997). Average mixed layer depths were 9 ± 8 m in 2010 and 9 ± 7 m in 2011. Bottom waters were defined as all waters within 5 m of the seafloor, and mid waters were defined as all waters between the mixed layer and bottom waters. Seventeen transects were analyzed, nine of which were sampled during both cruises (Fig. 1). Of the transects sampled, three in 2010 (Central Channel, Hanna Shoal North, and North Chukchi) and six in 2011 (Chukchi Slope Center, Chukchi Slope East, Chukchi Slope West, Hanna Shoal North, Hanna Shoal South East, and North Chukchi) contained winter water. The Barrow Canyon Center transect was chosen for direct comparison to the Bering Strait transect due to the Beaufort Shelf Jet outflow, and thus reflects the net alterations that occur to ocean waters as they enter and travel through the Chukchi Sea.

3.2. Water column Total P

Within the eastern Chukchi Sea (entire study area), the TP significantly increased from 2010 to 2011 (Tables 1 and 2), with significant shifts in nearly all of the P pools, with the exception of DOP. On average, TP was comprised of $48 \pm 17\%$ SRP, $37 \pm 17\%$ DOP, $12 \pm 7\%$ PIP and $12 \pm 7\%$ POP during 2010 and $58 \pm 17\%$ SRP, $34 \pm 15\%$ DOP, $9 \pm 5\%$ PIP and $9 \pm 5\%$ POP during 2011. Note that TP concentrations in bottom waters were higher than the waters above and remained relatively constant annually. In contrast, TP concentrations within the mixed layer and mid waters were lower, decreasing further in the mixed layer and increasing within the mid waters in 2011. (Tables 1 and 2).

Winter water TP concentrations were similar in 2010 and 2011 and consistently ~1.5 times greater than TP concentrations in non-winter waters. TP concentrations in ACC waters were also consistent between years, while offshore concentrations increased in 2011 relative to 2010 and inshore waters declined. As a result, ACC waters had lower or similar TP concentrations to inshore waters, and significantly lower TP concentrations than offshore waters during the 2010 cruise. The following year, however, TP concentrations increased significantly from inshore to ACC to offshore (Tables 1 and 2). There were no significant shifts in TP concentrations between water entering the Chukchi Sea (Bering Strait) and that leaving the region (Barrow Canyon Center).

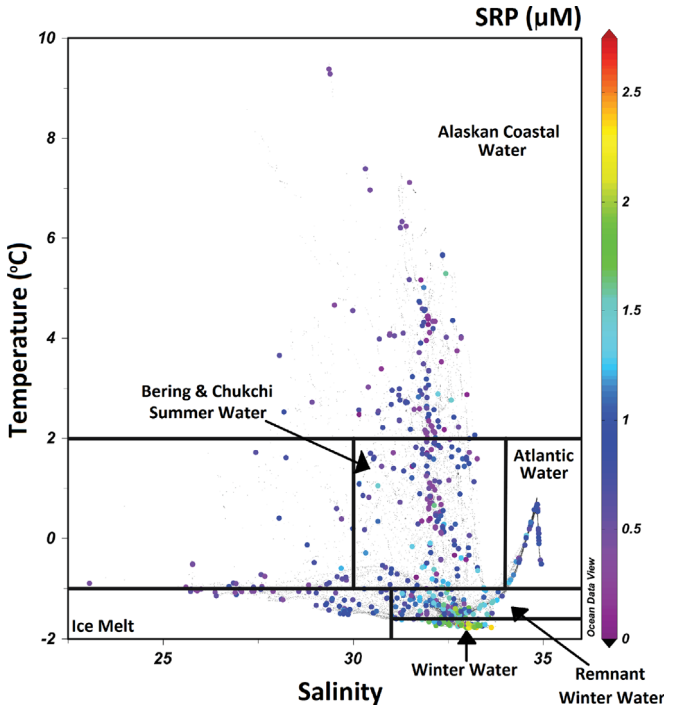

Fig. 2. Plot of Temperature versus Salinity accentuating separate water masses present in the eastern Chukchi Sea during the ICESCAPES mission. SRP concentrations are also provided for each sample.

3.3. Water column dissolved P

Dissolved P concentrations within the Chukchi Sea varied widely, with values that ranged from 0.45 to 3.48 μM in 2010 and from 0.39 to 3.61 μM in 2011. Both SRP and TDP increased with increasing depth, with average dissolved P concentrations significantly increasing from 2010 to 2011, predominantly due to an increase in SRP in mid-waters (Tables 1 and 2). Non-winter water was relatively constant between cruises, however winter water dissolved P concentrations were consistently higher than non-winter waters and increased from 2010 to 2011.

The dissolved P pool experienced significant shifts between regions as well. SRP increased with increasing distance from shore during 2010, and both SRP and TDP were significantly higher offshore in 2011. Within the ACC, SRP and TDP concentrations were elevated relative to that of inshore waters during 2011. The DOP pool in the 2010 offshore waters was also higher relative to the inshore waters, while 2011 DOP pools remained relatively stable across all regions. The 2010 TDP pool significantly increased offshore relative to ACC waters, but not relative to inshore waters. The 2011 TDP pool increased consistently with distance from shore (Tables 1 and 2). Finally no significant shifts in dissolved concentrations were noted between water entering the Chukchi Sea (Bering Strait $TDP_{2010} = 1.05 \pm 0.38$ μM, $TDP_{2011} = 1.09 \pm 0.50$ μM) and that leaving the region (Barrow Canyon Center $TDP_{2010} = 1.28 \pm 0.35$ μM, $TDP_{2011} = 1.18 \pm 0.45$ μM).

3.4. Water column particulate P

Particulate P concentrations within the Chukchi Sea were lower and more variable than their dissolved counterparts. TPP ranged from below detection in both years to a maximum of 1.44 μM in 2010 and 1.23 μM in 2011. The overall average TPP pool showed a significant decline from 2010 to 2011 with decreases in both the inorganic and organic phases (Tables 1 and 2). This reduction occurred in both the mixed layer and mid waters, though the

Please cite this article as: Piper, M.M., et al., Dissolved and particulate phosphorus distributions and elemental stoichiometry throughout the Chukchi Sea. Deep-Sea Res. II (2016), http://dx.doi.org/10.1016/j.dsr2.2016.05.009

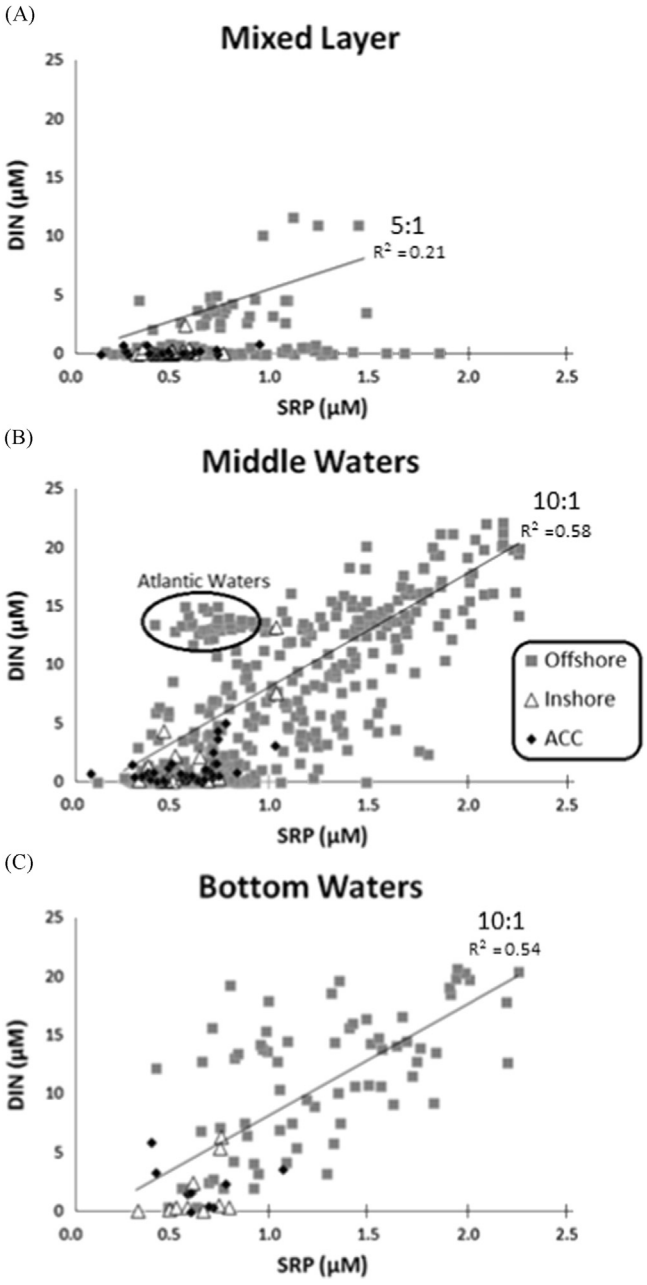

Fig. 3. DIN (μM) versus SRP (μM) relationships within the A. mixed layer, B. mid waters ($R^2=0.58$ excluding Atlantic waters), and C. bottom waters during both 2010 and 2011 ICESCAPE cruises. Offshore (gray squares), ACC (black diamonds), and Inshore (open triangles) waters are separated for comparison. Atlantic waters (see text) are circled. Best fit linear relationships includes all stations, and excludes samples with DIN below 2 μM. All p-values <0.01.

bottom waters remained relatively unchanged in both PIP and POP concentrations. Similar to the bottom waters, winter water also remained relatively constant between years; however, non-winter waters declined in TPP by nearly 50% in 2011. Annually, both inshore and offshore waters had significant decreases in the TPP pool. The inshore decline was predominantly driven by a reduction in POP, while both offshore PIP and POP concentrations decreased significantly from 2010 to 2011.

During the 2010 cruise, all forms of particulate P remained relatively uniform with depth. The following year, however, bottom waters contained significantly more TPP and PIP than mid and mixed waters, and more POP than mixed waters. Winter water TPP and PIP were the same as non-winter waters during 2010. The POP pool was elevated in non-winter waters, opposite of that observed during the 2011 cruise, when winter water had more than double POP concentrations of non-winter waters. The 2011 cruise also had significant increases in TPP and PIP within winter water relative to non-winter water.

Offshore particulate P concentrations were consistently higher than either inshore or ACC waters in all phases, regardless of year. During 2010 offshore waters contained more particulate P in all phases than ACC waters and more PIP than inshore waters. The following year, offshore waters held more particulate P in all phases than inshore waters, and more POP than both ACC and inshore waters. These elevations in particulate P concentrations were associated with significant increases in chlorophyll *a*, which averaged 5.66 ± 9.27 μg L^{-1} and 3.28 ± 0.63 μg L^{-1} in 2010 and 2011, respectively.

3.5. Water column elemental stoichiometry

In order to place P pool concentrations and distributions in perspective, dissolved and particulate P concentrations were compared to dissolved inorganic N ($DIN=NO_3^- + NO_2^- + NH_4^+$), POC, and PN concentrations with depth (mixed layer, mid waters, bottom waters) and with water mass (inshore, ACC, offshore) (Figs. 3 and 4). In the mixed layer (Fig. 3A), SRP concentrations were plentiful with respect to DIN in all inshore and ACC waters. Offshore waters had bimodal nutrient distributions, with most samples characterized by high SRP concentrations and below detection DIN, while a few samples were characterized by a DIN:SRP ratio of 5 and R^2 of 0.21 ($p<0.01$) between the two variables (Fig. 3). In the mid (Fig. 3B) and deep waters (Fig. 3C), N depletion was reduced, with a DIN:SRP ratio of 10:1 at both depths (mid waters, $R^2=0.58$; bottom waters, $R^2=0.54$, p values <0.01). In 2011, Atlantic waters were also sampled and were characterized by lower DIN:SRP ratios of 1.6:1 ($R^2=0.31$, $p<0.01$). There were no significant differences between sample years with regards to the DIN:SRP ratio ($p>0.05$). DIN and SRP ratios showed no significant changes between the Bering Strait and Barrow Canyon Center.

To understand particulate stoichiometry, POC and PN versus both POP and TPP concentrations were examined (Fig. 4). While TPP is typically assumed to be derived solely from biological activity in the open ocean, coastal waters are more complex due to terrigenous fluxes from the nearshore that may add non-living and mineral P (PIP) to the system (Benitez-Nelson, 2000). POP concentrations also underestimate biologically derived inorganic P components, such as polyphosphate (Hupfer et al., 2008).

Particulate elemental ratios varied both with depth and year, while remaining similar across water masses, although data were limited. Within the mixed layer, 69% of the variance in PN concentration was explained by changes in POC, with a POC:PN ratio of 8:1. With depth, this relationship moved closer to canonical Redfield (1958) ratios of 6.6:1. The POC:POP ratio was higher than the Redfield ratio at 173:1 ($R^2=0.42$, $p<0.01$); however, when the inorganic fraction was included (POC:TPP), the ratio decreased to 114:1 ($R^2=0.54$, $p<0.01$). A similar decline was observed for PN to particulate P ratios, with a PN:POP ratio of 13:1 ($R^2=0.32$, $p<0.01$) and PN:TPP ratio of 10:1 ($R^2=0.52$, $p<0.01$) (Fig. 4A and B). Samples collected during under ice blooms in 2010 and 2011 (Arrigo et al., 2012; Arrigo, 2014) differed from the bulk dataset and from one another, with significantly higher POC:PN:POP ratios of 898:52:1 (274:16:1, substituting TPP for POP) in 2010 and below detection POP (784:124:1, substituting TPP for POP) in 2011, suggesting rapid biological uptake and production of very labile organic matter.

Mid waters were characterized by lower POC:PN (7:1) and POC:POP (145:1) but higher PN:POP (Fig. 4A and C) ratios than those measured in the mixed waters and were consistent with preferential

Please cite this article as: Piper, M.M., et al., Dissolved and particulate phosphorus distributions and elemental stoichiometry throughout the Chukchi Sea. Deep-Sea Res. II (2016), http://dx.doi.org/10.1016/j.dsr2.2016.05.009

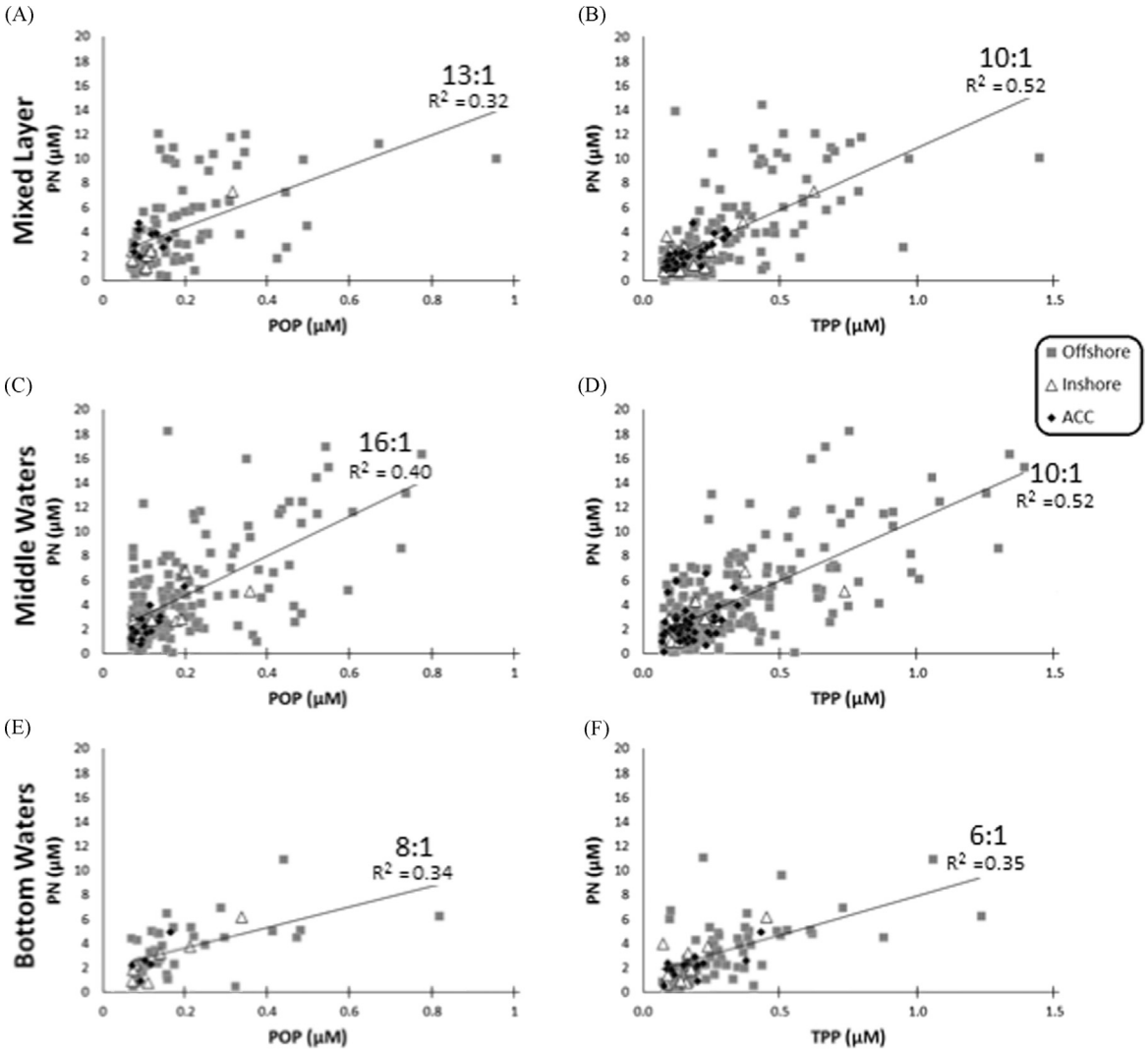

Fig. 4. PN (μM) versus POP (μM) relationships within the A. mixed layer, C. mid waters, and E. bottom waters, as well as PN (μM) versus TPP (μM) relationships within the B. mixed layer, D. mid waters, and F. bottom waters, during both ICESCAPE cruises. Offshore (gray squares), ACC (black diamonds), and Inshore (open triangles) waters are separated for comparison. All p-values < 0.01.

remineralization of P relative to N with increasing depth, even in this shallow sea. Mid water POC:TPP (87:1) was lower and PN:TPP similar to that measured in the mixed layer (Fig. 4B and D). There were no significant differences between the various water masses or with year. Bottom waters were characterized by significantly different elemental ratios than those found in the mixed layer and in mid waters, with lower C:N:P ratios ($R^2 = 0.34$, $p < 0.01$).

3.6. Sea Ice

Ice sampled within the Chukchi Sea during the 2010 cruise contained, on average, 0.67 ± 1.05 μM TPP and was evenly distributed between organic (0.34 ± 0.60 μM) and inorganic phases (0.33 ± 0.60 μM). Particulate P sampled in 2011 was an order of magnitude lower, with average TPP concentrations of 0.05 ± 0.03 μM. Dissolved P concentrations were only measured within the 2011 ice cores and averaged 0.38 ± 0.19 μM and was dominated by DOP (0.23 ± 0.18), with SRP concentrations significantly lower (0.15 ± 0.08 μM).

In order to understand the potential role of first year sea ice melt on the underlying water column, P inventories were determined within the entirety of each core compared to the nutrient inventories measured in the corresponding mixed layer of the sampled station. Mixed layer inventories were determined assuming a uniform depth of 5 m (average mixed layer depth below the ice pack was 5 ± 1 m in 2010 and 5 ± 4 m in 2011). Due to inter-station variability (Fig. 5A), TP inventories were only derived from samples in which all P forms were sampled from one core. As such, SRP and DOP concentrations collected during 2010 are not reported here.

Three ice cores in 2011 were sampled for both particulate and dissolved P resulting in average inventories of 6.23 ± 0.80 μmol SRP m^{-2} and 9.97 ± 4.42 μmol DOP m^{-2}, ranging from 5.69–7.15 μmol SRP m^{-2} and 5.60–14.45 μmol DOP m^{-2}. There were no clear patterns in P inventory or composition within each ice core (Fig. 5B). While average TDP and SRP inventories were significantly lower than underlying mixed layer waters ($p < 0.05$), average DOP inventories were similar. TPP and PIP inventories were significantly different between years (Fig. 5A). In 2010, particulate P inventories averaged 12.35 ± 12.93 μmol m^{-2} and 6.14 ± 7.86 μmol m^{-2} for TPP and PIP, respectively, while in 2011, inventories were more than 10 times lower, averaging 0.94 ± 0.47 μmol m^{-2} and 0.60 ± 0.23 μmol m^{-2}. These differences are likely due to sampling location (offshore in 2011, inshore in 2010) although temporal differences cannot be dismissed.

Please cite this article as: Piper, M.M., et al., Dissolved and particulate phosphorus distributions and elemental stoichiometry throughout the Chukchi Sea. Deep-Sea Res. II (2016), http://dx.doi.org/10.1016/j.dsr2.2016.05.009

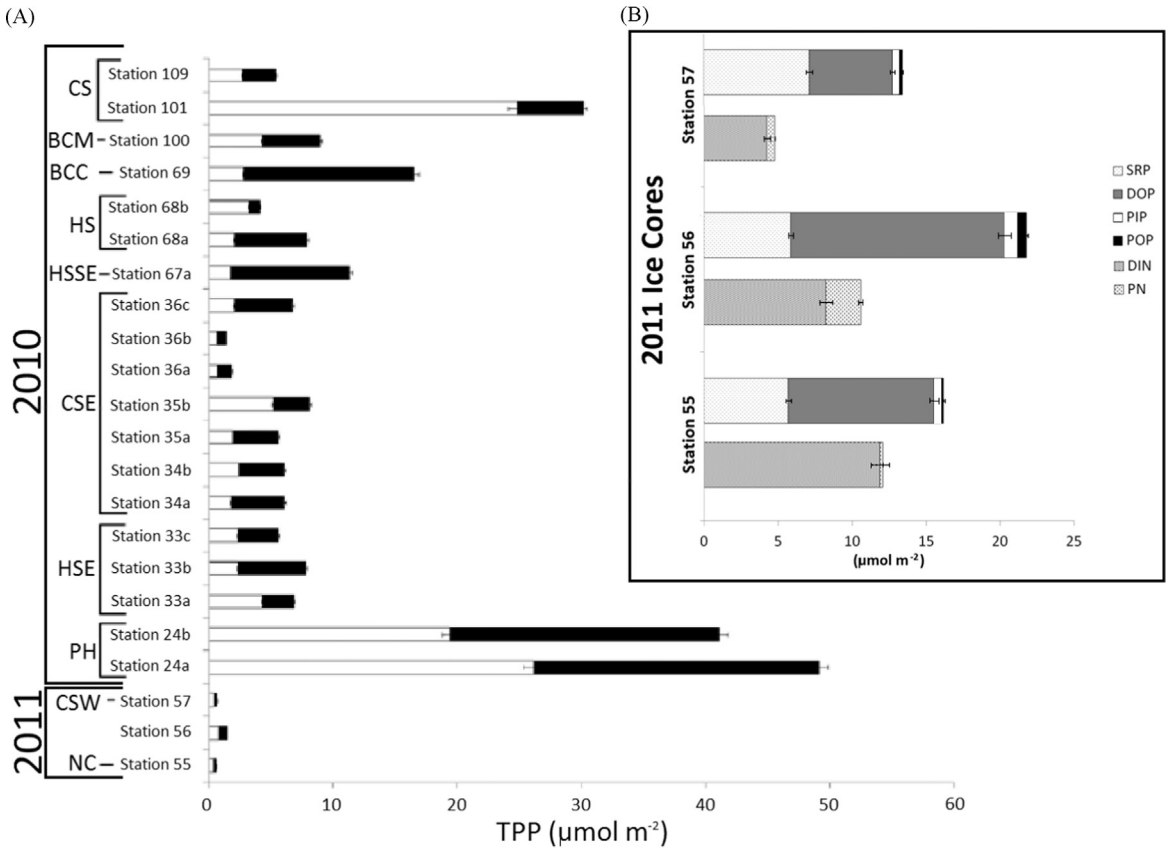

Fig. 5. (A) Total particulate P (μmol m^{-2}) inventories of ice cores collected during both 2010 and 2011 cruises. (B) Total P and TN (μmol m^{-2}) inventories for three ice core stations sampled during the 2011 cruise. Error bars represent propagated analytical errors. Note, the legend is the same for both (A) and (B) panels.

If all of the first year ice measured were to melt, TP inventories within the upper 5 m would decline to 28.45 ± 5.91 μmol m^{-2} (28% reduction). Average DOP inventories would decline the least, dropping by 0.28 μmol m^{-2} or 3% to 10.24 ± 0.99 μmol m^{-2}. Thus, much of the change that would occur in the TDP pool is driven by dilution of SRP, which would decline by 35% to 13.53 ± 3.68 μmol m^{-2}. In the particulate phases, both PIP and POP would decline by nearly 50%, to 2.49 ± 1.04 μmol m^{-2} and 2.20 ± 1.75 μmol m^{-2}, respectively. In contrast, while DIN inventories were much more variable, ice melt would result in an overall decrease of only 6%, to an average of 8.66 ± 6.57 μmol m^{-2}.

Nutrient ratios within the sea ice were analyzed by year and ice type (i.e., sediment-laden versus clean). Sediment-laden sea ice had substantially higher PC and PN concentrations and higher C:N:P ratios (456:31:1) compared to those of both 2010 clean ice (34:2:1) and 2011 clean ice (143:27:1). While all sea ice collected in 2011 had considerably lower nutrient concentrations, elemental ratios (168:30:1) were much closer to canonical Redfield (1958) ratios of 106:16:1.

4. Discussion

As P makes its way through the Chukchi Sea, farther into the Arctic Ocean, P concentrations and composition are influenced by a variety of processes that include river runoff, bottom resuspension, biological activity, and sea ice formation and melt. Most of these processes were evident during the 2010 and 2011 sampling periods, and caused significant regional variability.

4.1. Riverine inputs and bottom resuspension

Given the coastal nature of our sampling, riverine inputs are expected to supply significant P to the Chukchi Sea (e.g., Galloway et al., 1996, Ruttenberg, 2003), particularly via Kotzebue Sound. There is little information on the nutrient composition of the rivers feeding directly into the Chukchi (e.g., the Noatak, Selawik, and Kobuk Rivers); however the composition is likely similar to the larger rivers fed from Alaska, such as the Yukon and Mackenzie Rivers. Both the Yukon and Mackenzie Rivers supply relatively little P (average fluxes of 1.9×10^9 and 1.5×10^9 g P y^{-1}) with respect to N (average fluxes of $19–24 \times 10^9$ and $12.5–24 \times 10^9$ g N y^{-1}) to the coastal ocean, with dissolved N:P ratios of about 10–13 and 8–16, respectively (Le Fouest et al., 2013). Our study indicates that riverine inputs are also relatively small, with little evidence of riverine P being supplied to the water column of the Chukchi Sea during sampling.

Average inorganic P concentrations inshore were consistently lower than offshore waters, regardless of year (Tables 1 and 2). Furthermore, there was no clear evidence of high particulate P inshore relative to offshore regions, suggesting that if the source of particulate P was continental discharge (via rivers, groundwater, or other mechanisms), it was rapidly removed from the system (Ruttenberg, 2003, Benitez-Nelson, 2000). In the examination of a sediment core located near the Icy Cape transect, Zhang et al. (2010) found particulate N:P ratios of ~1.6 when inorganic P was included; however, the ratio increased substantially to 14.2 when only the organic fraction was used to determine the ratio. This result, coupled with their findings that the inorganic P phases (comprised of detrital, authigenic, and oxide associated P) were more than 85% of the P pool, suggest that continental runoff does supply P to the inshore system, but that these particles are rapidly

Please cite this article as: Piper, M.M., et al., Dissolved and particulate phosphorus distributions and elemental stoichiometry throughout the Chukchi Sea. Deep-Sea Res. II (2016), http://dx.doi.org/10.1016/j.dsr2.2016.05.009

removed near shore. Thus, regional comparisons of dissolved and particulate P concentrations across the eastern Chukchi Sea suggest that riverine input had a relatively minor impact on water column P biogeochemistry during the time of sampling.

Although Alaskan continental discharge did not appear to be a major source of P to the Chukchi Sea water column during the ICESCAPE cruises, it is important to note that this is likely not the case for all Arctic rivers. The Arctic Ocean receives more than 10% of global riverine discharge, though it only accounts for approximately 1% of the world's ocean by volume (Menard and Smith, 1966, Aagaard and Carmack, 1989). The Ob River in particular supplies almost an order of magnitude more than the riverine input of the Mackenzie and Yukon Rivers combined, with average P fluxes of 17–21.3 $\times$ 10^9 g P y^{-1} and N:P ratios of 0.5–1.5 (Gordeev et al., 1996; Holmes et al., 2000; Dittmar and Kattner, 2003; Gordeev and Kravchishina, 2009; Holmes et al., 2011).

Results from Zhang et al. (2010), and the shallow nature of the Chukchi Sea, suggest that bottom resuspension may also be an important source of recycled P to the Chukchi Sea. While there was little evidence of resuspension during the 2010 cruise (less than 20% of bottom water samples had elevated particulate P in comparison to mid waters), the 2011 cruise found significant increases in all particulate P phases within bottom waters. The particulate P increase during 2011 suggests that resuspension may play an important role in P dynamics, at least periodically. Souza et al. (2014b) found a significant efflux of dissolved P from sediments at stations located within the inshore and offshore regions of the Chukchi Sea (see Section 3.1), but also found uptake of SRP in sediments located within the ACC. They argued that the P uptake was reduced in the other regions due to the availability of other limiting nutrients, namely N. Increases in dissolved P concentrations were also noted with increasing depth; however, our sampling did not allow us to determine whether the P increase was due to bottom resuspension, regeneration of P from sediments, or remineralization of P from sinking material from above.

4.2. Biology

Phosphorus plays a key role in a number of biochemical reactions within marine systems by influencing biological production as well as community composition and food web structure (Karl, 2014). In order to understand the potential role of P in the Chukchi Sea, both N and C must be considered as well. For decades, the concept that all marine phytoplankton have a fixed “Redfield” C, N, to P ratio has been the foundation of numerous studies that examine carbon and nutrient biogeochemistry in marine systems. In essence, any deviation in the elemental ratios of C, N, and P from canonical Redfield ratios is often used to determine nutrient limitation or stress (Redfield, 1958, Tyrrell, 1999). However, the relationships between these elements are often decoupled, particularly in nearshore regimes, owing to changes in nutrient source, food web dynamics, and physical forcing (Karl et al., 1997, Weber and Deutsch, 2010, Martin et al., 2014).

During both the 2010 and 2011 ICESCAPE cruises within the Chukchi Sea, dissolved and particulate N:P ratios were variable (Figs. 3 and 4). In the mixed layer, dissolved N concentrations for most of our study region were below detection (Fig. 4A and B), suggesting strong N limitation, consistent with other work (Cota et al., 1996, Mills et al., 2015). Only in offshore waters and with increasing depth did significant dissolved nutrient relationships begin to emerge (Fig. 4C–F). When DIN was exhausted in surface waters, SRP concentrations remained high, averaging 1.30 μM, with an N:P ratio < 2. This indicates there is a significant source of excess dissolved P that leaves the Chukchi Sea within the surface waters, and is potentially a major source of P to surface waters of the Arctic Ocean (consistent with Yamamoto-Kawai et al., 2006). Indeed, recent studies suggest that the Arctic Ocean as a whole is a net exporter of phosphate (unfiltered SRP) ($\sim$1.0 $\pm$ 0.3 kmol P s^{-1}, net $\pm$ 1 std error) to the North Atlantic relative to N (Danielson et al., 2011, Torres-Valdés et al., 2013). Furthermore, their P measurements ignore organic P, and therefore likely underestimate the magnitude of P exiting the Arctic Ocean. It is important to note that the SRP concentrations entering the Bering Strait during the sampling period of Torres-Valdés et al. (2013) are either similar to, or lower than those observed during the ICESCAPE cruises. Such low dissolved N:P ratios within surface waters leaving the Chukchi Sea provide an ideal environment for N fixation, and are likely contributing to the magnitude of N fixation in the northern Atlantic Ocean hypothesized to be a result of Arctic outflow (Yamamoto-Kawai et al., 2006).

Significant correlations between all SRP and DIN concentration data emerge deeper in the water column, most likely due to the remineralization of sinking organic matter (Fig. 3). DIN:SRP ratios in offshore mixed layer and mid waters throughout the Chukchi Sea ranged from 7–9.1, consistent with biological activity associated with low N:P sinking material (see below and Martiny et al., 2013), or removal of DIN via denitrification (Mills et al., 2015). Similar ratios were presented in the Souza et al. (2014) study of N:P within the surface and bottom waters throughout the Chukchi Sea. They found dissolved inorganic surface water N:P ratios varying between 0.4–3.5 and deep water N:P ratios ranging from 6–15.

Particulate N:P ratios were also quite variable throughout the Chukchi Sea (Fig. 4). It is now recognized that various groups of marine phytoplankton have N:P ratios that span a factor of 5 or more (Liu et al., 2004, Zhang et al., 1996, Martiny et al., 2013). Most of this N:P plasticity is attributed to the ability of cyanobacteria to utilize N_2 from the atmosphere for their nutritional N needs (e.g., N_2 fixation) as well as the bioaccumulation of inorganic and oxidized organic P forms that contain minimal N (e.g., polyphosphate or phospholipids) even during times when dissolved P concentrations are quite low (< 0.05 μM) (Orchard et al., 2010, Martin et al., 2014). Martiny et al. (2013) presented a global compilation of particulate C:N:P ratios and found significantly lower ratios of 78:13:1 within the polar regions. These low C:N:P ratios are generally associated with high diatom abundances (Hill et al., 2005) and are expected given the abundant diatom community present within the Chukchi Sea during the 2010–2011 sampling periods (Laney and Sosik, 2014). Particulate N:P ratios during the ICESCAPE cruises range from 6:1 to 16:1 depending on depth and the form of particulate P used in the elemental ratio analysis.

4.3. The role of sea ice

Sea Ice has both direct and indirect impacts on nutrient biogeochemistry in the Chukchi Sea. Indirect impacts include the formation of nutrient rich underlying waters during brine ejection as sea ice forms (PWW), changes in the magnitude of light penetration with sea ice presence, and subsequent potential enrichment of nutrients to underlying waters upon sea ice melt. Both ICESCAPE cruises encountered stations that encompassed PWW (Fig. 2). These waters, formed during sea ice formation, are enriched in nutrients and hypothesized to drive water column primary production within the Chukchi Sea (Lowry et al., 2015). This study shows that PWW does indeed contain significantly more SRP (Fig. 2) and DIN (Tables 1 and 2) relative to non-winter waters within the same regions, with SRP concentrations increasing by more than 50%. Our results, coupled with the location of chlorophyll *a* hot spots near PWW shown by Lowry et al. (2015), indicate that not only is PWW a potential driver of spring and early summer blooms, but that the remnants of PWW may continue to fuel additional blooms throughout the season. Closer examination

Please cite this article as: Piper, M.M., et al., Dissolved and particulate phosphorus distributions and elemental stoichiometry throughout the Chukchi Sea. Deep-Sea Res. II (2016), http://dx.doi.org/10.1016/j.dsr2.2016.05.009

of nutrient ratios indicate that the average DIN:SRP was 8.8 and was similar to that found in other Chukchi Sea deep waters.

A combination of increased water temperatures entering the Chukchi Sea, changes in warm Pacific water movement within the Chukchi Sea (Shimada et al., 2006; Woodgate et al., 2006, Mizobata et al., 2010; Brugler et al., 2014), increases in poleward wind forcing (Wu et al., 2006; Wang et al., 2009; Overland et al., 2012) and alterations in the Arctic and Pacific Decadal Oscillations (Wang and Ikeda 2000; Rigor et al., 2002; Liu et al., 2004; Zhang et al., 2010; Stroeve et al., 2011; Danielson et al., 2011; Wendler et al., 2014) have all led to increased sea ice melt that occurs at variable times earlier in the year within the Chukchi Sea (Frey et al., 2015). In fact, most of the sea ice that occurs within the Chukchi Sea is thinner first year ice rather than thicker multi-year ice, a transition that is occurring throughout most of the Arctic Ocean and particularly in the Pacific sector (Maslanik et al., 2011). Between the 2010 and 2011 ICESCAPE cruises, 2011 ice melt occurred earlier in the season, allowing for the cruise to extend farther north. Earlier ice melt, however, resulted in a lack of sea ice within close proximity to shore. These differences in ice melt timing and sample location are likely a key component of the large scale variability in nutrient concentrations observed throughout the ICESCAPE project.

In 2010, sea ice contained particulate P concentrations as much as 35 times higher than those measured in 2011 (Fig. 5A). In 2010, sea ice cores were collected much closer to land and many were visibly more sediment laden. Although highly variable, the range of P concentrations measured in the Chukchi Sea ice cores is similar to that measured elsewhere and in first year sea ice (Gradinger, 2009).

Observed core to core and within core variability in nutrient concentrations are not unexpected as sea ice, particularly within the relatively shallow Chukchi Sea shelf, may come in contact with the seafloor during formation and incorporate both benthic biota and sediments (Gradinger and Ikävalko, 1998). Sea ice P content is also a function of the water depth at which sea ice was formed (Reimnitz et al., 1992), the magnitude and composition of dust and snow inputs (Ehn et al., 2004, Nomura et al., 2011), the occurrence of melt ponds that may contain biological activity, and biological production within the ice itself (Garrison et al., 1986, Gradinger and Ikävalko 1998, Arrigo, 2014). As a result, variable sea ice nutrient concentrations, (i.e., sediment laden versus “clean” ice) may have very different impacts on the surrounding environment when sea ice melts.

In 2010, average sediment laden sea ice particulate C:N:P ratios of 456:31:1 were significantly higher than traditional Redfield ratios, falling between marine ratios and those generally found in terrestrial environments (McGroddy et al., 2004), suggesting terrestrial organic matter may have been a significant source of material. During the same cruise, clean sea ice nutrient ratios were much lower (34:2:1) and suggests *in situ* algal production and remineralization (Krembs et al., 2002, Gradinger, 2009). In 2011, particulate nutrient concentrations within the offshore sea ice were considerably lower with C:N:P nutrient ratios (168:30:1), again more similar to Redfield. Lower particulate nutrient concentrations suggests that *in situ* algal production and remineralization were a dominant process within the 2011 sea ice cores.

During the ICESCAPE cruises, phytoplankton blooms occurred under the sea ice (Arrigo et al., 2012). In order to estimate the potential role of nutrients in sea ice melt on water column biological production within the region, we calculated an inventory of sea ice nutrients (using 2011 data) and assumed that all of the sea ice melted into the mixed layer of underlying waters. Our results suggest that rather than adding net nutrients, sea ice melt actually dilutes water column nutrient concentrations and is much more significant for SRP (average decline of 35%) relative to DIN (6% decline). Given that Chukchi Sea blooms are likely N-limited (Wendler et al., 2014, Arrigo et al., 2012, Mills et al., 2015), nutrients within sea ice melt neither promote nor inhibit blooms; however, it may impact biological diversity, at least on a transient basis, of responding organisms as ice melt expands. It is important to note here that these dilution estimates do not take into account the potential release and solubilization of TPP that also enters underlying waters upon ice melt.

5. Conclusions

The Chukchi Sea is undergoing large scale ecosystem changes due to rising water temperatures, melting sea ice, and changes in current patterns (Brugler et al., 2014). As this sea is a major pathway by which nutrient-rich Pacific waters make their way into the Arctic, changes in Chukchi Sea biogeochemistry have the potential to influence Arctic Ocean waters as well. Results from the ICESCAPE cruises suggest that the eastern Chukchi Sea currently serves as a major source of both inorganic and organic P to the rest of the Arctic Ocean, and that much of the P that enters the Chukchi Sea is biologically modified during transit. While rivers are likely a significant source of P elsewhere in the Arctic Ocean, increased riverine discharge within the Chukchi Sea results in minimal additions to water column P. Furthermore, while the Chukchi Sea is a shallow sea, there was little evidence of P inputs from sediments. Finally, while sediment laden sea ice melt associated with nearshore waters may potentially add significant P to coastal waters, offshore sea ice melt will likely result in a significant reduction of water column P concentrations due to freshwater dilution. In contrast, ice formation leads to substantially enhanced SRP concentrations that may help to fuel phytoplankton blooms.

The Chukchi Sea is light limited during the winter and nitrogen limited during the spring and summer months. With warmer temperatures, ice melt will continue to increase, enabling increased phytoplankton growth earlier in the year, but ultimately reducing dissolved P concentrations via a reduction in PWW formation and sea ice melt. At the same time, stronger stratification is also hypothesized to occur due to strengthening northeasterly winds (Brugler et al., 2014). Reduced water column mixing may further promote rates of denitrification in the mid waters exacerbating N removal (Mills et al., 2015). Finally, the strength of the ACC and Beaufort Jet are predicted to decline in coming years due to changes in wind strength (Brugler et al., 2014). We hypothesize that due to reduced upwelling, N-limitation, increasing rates of denitrification, and elevated P pools within offshore waters, the eastern Chukchi Sea will continue to provide and be an increasing source of “excess” P to other regions of the Arctic Ocean.

Acknowledgments

This work would not have been possible without the support provided by NASA ICESCAPE Grants NNX09AE42G and NNX09AE65G and NASA Cryospheric Sciences Program (Grants NNX10AH71G and NNX14AH61G). We would also like to extend our gratitude to all aboard the USCGC *Healy* during the ICESCAPE mission. A special thank you also goes to Dr. Kevin Arrigo, for leading the ICESCAPE mission and Wendy Plessinger and Melissa Bennett for their assistance in P analyses.

References

Aagaard, K., Carmack, E.C., 1989. The role of sea ice and other fresh water in the Arctic circulation. J. Geophys. Res. 94 (C10), 14485–14498.

Armstrong, F.A.J., Stearns, C.R., Strickland, J.D.H., 1967. The measurement of upwelling and subsequent biological process by means of the Technicon Autoanalyzer® and associated equipment. Deep. Sea Res. Ocean. Abstr. 14, 381–389.

Arnell, N.W., 2005. Implications of climate change for freshwater inflows to the Arctic Ocean. J. Geophys. Res.: Atmos. 1984–2012, 110.

Arrigo, K.R., 2014. Sea ice ecosystems. Annu. Rev. Mar. Sci. 6, 439–467.

Arrigo, K.R., Perovich, D.K., Pickart, R.S., Brown, Z.W., van Dijken, G.L., Lowry, K.E., Mills, M.M., Palmer, M.A., Balch, W.M., Bahr, F., Bates, N.R., Benitez-Nelson, C., Bowler, B., Brownlee, E., Ehn, J.K., Frey, K.E., Garley, R., Laney, S.R., Lubelczyk, L., Mathis, J., Matsuoka, A., Mitchell, B.G., Moore, G.W.K., Ortega-Retuerta, E., Pal, S., Polashenski, C.M., Reynolds, R.A., Schieber, B., Sosik, H.M., Stephens, M., Swift, J.H., 2012. Massive Phytoplankton blooms under Arctic Sea ice. Science 336, 1408.

Arrigo, K.R., van Dijken, G.L., 2011. Secular trends in Arctic Ocean net primary production. J. Geophys. Res.: Oceans 1978–2012, 116.

Arrigo, K.R., van Dijken, G.L., 2015. Continued increases in Arctic Ocean primary production. Progress. Oceanogr.

Aspila, K.I., Agemian, H., Chau, A.S.Y., 1976. A semi-automated method for the determination of inorganic, organic and total phosphate in sediments. Analyst 101, 187–197.

Benitez-Nelson, C., O'Neill, L., Kolowith, L.C., Pellechia, P., Thunell, R., 2004. Phosphonates and particulate organic phosphorus cycling in an anoxic marine basin. Limnol. Ocean. 49, 1593–1604.

Benitez-Nelson, C.R., 2000. The biogeochemical cycling of phosphorus in marine systems. Earth-Sci. Rev. 51, 109–135.

Benitez-Nelson, C.R., Madden, L.P.N., Styles, R.M., Thunell, R.C., Astor, Y., 2007. Inorganic and organic sinking particulate phosphorus fluxes across the oxic/anoxic water column of Cariaco Basin, Venezuela. Mar. Chem. 105, 90–100.

Bernhardt, H., Wilhelms, A., 1967. The continuous determination of low level iron, soluble phosphate and total phosphate with the AutoAnalyzer. InTech. Symp., 385–389.

Brown, Z.W., Casciotti, K.L., Pickart, R.S., Swift, J.H., Arrigo, K.R., 2015. Aspects of the marine nitrogen cycle of the Chukchi Sea shelf and Canada Basin. Deep. Sea Res. Part II: Top. Stud. Ocean.

Brugler, E.T., Pickart, R.S., Moore, G., Roberts, S., Weingartner, T.J., Statscewich, H., 2014. Seasonal to interannual variability of the Pacific water boundary current in the Beaufort Sea. Progress. Oceanogr. 127, 1–20.

Cooney, R., Coyle, K., 1982. Trophic implications of cross-shelf copepod distributions in the southeastern Bering Sea. Mar. Biol. 70, 187–196.

Cota, G., Pomeroy, L., Harrison, W., Jones, E., Peters, F., Sheldon Jr, W., Weingartner, T., 1996. Nutrients, primary production and microbial heterotrophy in the southeastern Chukchi Sea: Arctic summer nutrient depletion and heterotrophy. Mar. Ecol. Progress Ser. 135, 247–258.

Danielson, S., Curchitser, E., Hedstrom, K., Weingartner, T., Stabeno, P., 2011. On ocean and sea ice modes of variability in the Bering Sea. J. Geophys. Res.: Ocean. 1978–2012, 116.

Dittmar, T., Kattner, G., 2003. The biogeochemistry of the river and shelf ecosystem of the Arctic Ocean: a review. Mar. Chem. 83, 103–120.

Dyhrman, S., Chappell, P., Haley, S., Moffett, J., Orchard, E., Waterbury, J., Webb, E., 2006. Phosphonate utilization by the globally important marine diazotroph Trichodesmium. Nature 439, 68–71.

Ehn, J., Granskog, M.A., Reinart, A., Erm, A., 2004. Optical properties of melting landfast sea ice and underlying seawater in Santala Bay, Gulf of Finland. J. Geophys. Res.: Ocean. 1978–2012, 109.

Frey, K.E., Comiso, J.C., Cooper, L.W., Gradinger, R.R., Grebmeier, J.M., Saitoh, S.-I., Tremblay, J.-É., 2014. Arctic Ocean Primary Productivity, In: Arctic Report Card 2014. ⟨http://www.arctic.noaa.gov/reportcard⟩.

Frey, K.E., Moore, G., Cooper, L.W., Grebmeier, J.M., 2015. Divergent patterns of recent sea ice cover across the Bering, Chukchi, and Beaufort Seas of the Pacific Arctic Region. Progress Ocean.

Galloway, J., Howarth, R., Michaels, A., Nixon, S., Prospero, J., Dentener, F., 1996. Nitrogen and phosphorus budgets of the North Atlantic Ocean and its watershed. Springer, pp. 3–25.

Garrison, D.L., Sullivan, C.W., Ackley, S.F., 1986. Sea ice microbial communities in Antarctica. BioScience, 243–250.

Gong, D., Pickart, R.S., 2015. Summertime circulation in the eastern Chukchi Sea. Deep. Sea Res. Part II: Top. Stud. Ocean.

Gordeev, V.V., Kravchishina, M.D., 2009. River flux of dissolved organic carbon (DOC) and particulate organic carbon (POC) to the Arctic Ocean: what are the consequences of the global changes? In: Nihoul, J.C.J, Kostianoy, A.G. (Eds.) Incluence of Climate Change on the Changing Arctic and Subarctic Conditions. pp. 145–160.

Gordeev, V.V., Martin, J.M., Sidorov, I.S., Sidorova, M.V., 1996. A reassessment of the Eurasian river input of water, sediment, major elements and nutrients to the Arctic Ocean. J. Am. Sci. 296, 664–691.

Gosselin, M., Levasseur, M., Wheeler, P.A., Horner, R.A., Booth, B.C., 1997. New measurements of phytoplankton and ice algal production in the Arctic Ocean. Deep. Sea Res. Part II: Top. Stud. Oceanogr. 44, 1623–1644.

Gradinger, R., 2009. Sea-ice algae: major contributors to primary production and algal biomass in the Chukchi and Beaufort Seas during May/June 2002. Deep. Sea Res. Part II: Top. Stud. Oceanogr. 56, 1201–1212.

Gradinger, R., Ikävalko, J., 1998. Organism incorporation into newly forming Arctic sea ice in the Greenland Sea. J. Plankton Res. 20, 871–886.

Grebmeier, J.M., 2012. Shifting patterns of life in the Pacific Arctic and sub-Arctic Seas. Mar. Sci., 4.

Holland, M.M., Bitz, C.M., Tremblay, B., 2006. Future abrupt reductions in the summer Arctic sea ice. Geophys. Res. Lett., 33.

Holm-Hansen, O., Lorenzen, C.J., Holmes, R.W., Strickland, J.D., 1965. Fluorometric determination of chlorophyll. J. Cons. 30, 3–15.

Holmes, R.M., McClelland, J.W., Peterson, B.J., Tank, S.E., Bulygina, E., Egliton, T.I., Gordeev, V.V., Gurtovaya, T.Y., Raymond, P.A., Repeta, D.J., Staples, R., Striegl, R. G., Zhulidov, A.V., Zimov, S.A., 2011. Seasonal and annual fluxes of nutrients and organic matter from large rivers to the Arctic Ocean and Surrounding Seas. Estuaries Coasts 35 (2), 369–382.

Holmes, R., Peterson, B., Gordeev, V., Zhulidov, A., Meybeck, M., Lammers, R., Vörösmarty, C., 2000. Flux of nutrients from Russian rivers to the Arctic Ocean: Can we establish a baseline against which to judge future changes? Water Resour. Res. 36, 2309–2320.

Huang, X.-L., Zhang, J.-Z., 2010. Spatial variation in sediment-water exchange of phosphorus in Florida Bay: AMP as a model organic compound. Environ. Sci. Technol. 44, 7790–7795.

Hupfer, M., Glöss, S., Schmieder, P., Grossart, H.-P., 2008. Methods for detection and quantification of polyphosphate and polyphosphate accumulating microorganisms in Aquatic Sediments. Int. Rev. Hydrobiol. 93, 1–30.

Karl, D., Letelier, R., Tupas, L., Dore, J., Christian, J., Hebel, D., 1997. The role of nitrogen fixation in biogeochemical cycling in the subtropical North Pacific Ocean. Nature 388, 533–538.

Karl, D.M., 2014. Microbially mediated transformations of phosphorus in the sea: new views of an old cycle. Annu. Rev. Mar. Sci. 6, 279–337.

Kérouel, R., Aminot, A., 1997. Fluorometric determination of ammonia in sea and estuarine waters by direct segmented flow analysis. Mar. Chem. 57, 265–275.

Koroleff, F., 1983. Simultaneous oxidation of nitrogen and phosphorus compounds by persulfate. Methods Seawater Anal. 2, 205–206.

Krembs, C., Eicken, H., Junge, K., Deming, J.W., 2002. High concentrations of exopolymeric substances in Arctic winter sea ice: implications for the polar ocean carbon cycle and cryoprotection of diatoms. Deep. Sea Res. Part I: Ocean. Res. Pap. 49, 2163–2181.

Laney, S.R., Sosik, H.M., 2014. Phytoplankton assemblage structure in and around a massive under-ice bloom in the Chukchi Sea. Deep. Sea Res. Part II: Top. Stud. Oceanogr. 105, 30–41.

Le Fouest, V., Babin, M., Tremblay, J.E., 2013. The fate of riverine nutrients on Arctic shelves. Biogeosciences 10, 3661–3677.

Lilliefors, H.W., 1967. On the Kolmogorov–Smirnov test for normality with mean and variance unknown. J. Am. Stat. Assoc. 62, 399–402.

Liu, J., Curry, J.A., Hu, Y., 2004. Recent Arctic sea ice variability: connections to the Arctic Oscillation and the ENSO. Geophys. Res. Lett., 31.

Lowry, K.E., Pickart, R.S., Mills, M.M., Brown, Z.W., van Dijken, G.L., Bates, N.R., Arrigo, K.R., 2015. The influence of winter water on phytoplankton blooms in the Chukchi Sea. Deep. Sea Res. Part II: Top. Stud. Oceanogr. 118, 53–72.

Martin, P., Dyhrman, S.T., Lomas, M.W., Poulton, N.J., Van Mooy, B.A., 2014. Accumulation and enhanced cycling of polyphosphate by Sargasso Sea plankton in response to low phosphorus. Proc. Natl. Acad. Sci. 111, 8089–8094.

Martiny, A.C., Pham, C.T., Primeau, F.W., Vrugt, J.A., Moore, J.K., Levin, S.A., Lomas, M. W., 2013. Strong latitudinal patterns in the elemental ratios of marine plankton and organic matter. Nat. Geosci. 6, 279–283.

Maslanik, J., Stroeve, J., Fowler, C., Emery, W., 2011. Distribution and trends in Arctic sea ice age through spring 2011. Geophys. Res. Lett. 38.

McGroddy, M.E., Daufresne, T., Hedin, L.O., 2004. Scaling of C:N:P Stoichiometry in forests worldwide: Implications of terrestrail Redfield-type ratios. Ecology 85, 2390–2401.

McTigue, N.D., Bucolo, P., Liu, Z., Dunton, K.H., 2015. Pelagic-benthic coupling, food webs, and organic matter degradation in the Chukchi Sea: insights from sedimentary pigments and stable carbon isotopes. Limnol. Ocean. 60, 429–445.

Mills, M.M., Brown, Z.W., Lowry, K.E., van Dijken, G.L., Becker, S., Pal, S., Benitez-Nelson, C.R., Downer, M.M., Strong, A.L., Swift, J.H., 2015. Impacts of low phytoplankton NO^{3-}:PO_4^{3-} utilization ratios over the Chukchi Shelf, Arctic Ocean. Deep. Sea Res. Part II: Top. Stud. Oceanogr.

Mizobata, K., Shimada, K., Woodgate, R., Saitoh, S.-I., Wang, J., 2010. Estimation of heat flux through the eastern Bering Strait. J. Oceanogr. 66, 405–424.

Monaghan, E., Ruttenberg, K., 1999. Dissolved organic phosphorus in the coastal ocean: reassessment of available methods and seasonal phosphorus profiles from the Eel River Shelf. Limnol. Ocean. 44, 1702–1714.

Monterey, G., Levitus, S., 1997. Climatological Cycle of Mixed Layer Depth in the World Ocean. US Government Printing Office, NOAA NESDIS, p. 5.

Menard, H.W., Smith, S.M., 1966. Hypsometry of ocean basin provinces. J. Geophys. Res. 71, 4305–4325.

Mortazavil, B., Iversonl, R.L., Landing, W.M., Huang, W., 2000. Phosphorus budget of Apalachicola Bay: a river-dominated estuary in the northeastern. Mar. Ecol. Prog. Ser. 198, 33–42.

Münchow, A., Weingartner, T.J., Cooper, L.W., 1999. The summer hydrography and surface circulation of the East Siberian shelf sea. J. Phys. Oceanogr. 29, 2167–2182.

Nikolopoulos, A., Pickart, R.S., Fratantoni, P.S., Shimada, K., Torres, D.J., Jones, E.P., 2009. The western Arctic boundary current at 152 W: Structure, variability, and transport. Deep. Sea Res. Part II: Top. Stud. Oceanogr. 56, 1164–1181.

Nomura, D., McMinn, A., Hattori, H., Aoki, S., Fukuchi, M., 2011. Incorporation of nitrogen compounds into sea ice from atmospheric deposition. Mar. Chem. 127, 90–99.

Orchard, E.D., Benitez-Nelson, C.R., Pellechia, P.J., Lomas, M.W., Dyhrman, S.T., 2010. Polyphosphate in Trichodesmium from the low-phosphorus Sargasso Sea. Limnol. Oceanogr. 55, 2161–2169.

Please cite this article as: Piper, M.M., et al., Dissolved and particulate phosphorus distributions and elemental stoichiometry throughout the Chukchi Sea. Deep-Sea Res. II (2016), http://dx.doi.org/10.1016/j.dsr2.2016.05.009

Overland, J.E., Francis, J.A., Hanna, E., Wang, M., 2012. The recent shift in early summer Arctic atmospheric circulation. Geophys. Res. Lett., 39.
Paytan, A., McLaughlin, K., 2007. The oceanic phosphorus cycle. Chem. Rev. 107, 563–576.
Petrenko, D., Pozdnyakov, D., Johannessen, J., Counillon, F., Sychov, V., 2013. Satellite-derived multi-year trend in primary production in the Arctic Ocean. Int. J. Rem. Sens. 34, 3903–3937.
Pickart, R.S., 2004. Shelfbreak circulation in the Alaskan Beaufort Sea: mean structure and variability. J. Geophys. Res.: Oceans 1978–2012, 109.
Post, E., Bhatt, U.S., Bitz, C.M., Brodie, J.F., Fulton, T.L., Hebblewhite, M., Kerby, J., Kutz, S.J., Stirling, I., Walker, D.A., 2013. Ecological consequences of sea-ice decline. Science 341, 519–524.
Redfield, A.C., 1958. The biological control of chemical factors in the environment. Am. Sci. 230A, 221.
Reimnitz, E., Marincovich Jr, L., McCormick, M., Briggs, W., 1992. Suspension freezing of bottom sediment and biota in the Northwest Passage and implications for Arctic Ocean sedimentation. Can. J. Earth Sci. 29, 693–703.
Rigor, I.G., Wallace, J.M., Colony, R.L., 2002. Response of sea ice to the Arctic oscillation. J. Clim. 15, 2648–2663.
Ruttenberg, K., 2003. The global phosphorus cycle. Treatise Geochem. 8, 585–643.
Schumacher, J., Reed, R., 1986. On the Alaska coastal current in the western Gulf of Alaska. J. Geophys. Res.: Oceans 1978–2012 (91), 9655–9661.
Serreze, M.C., Holland, M.M., Stroeve, J., 2007. Perspectives on the Arctic's shrinking sea-ice cover. Science 315, 1533–1536.
Shimada, K., Carmack, E.C., Hatakeyama, K., Takizawa, T., 2001. Varieties of shallow temperature maximum waters in the western Canadian Basin of the Arctic Ocean. Geophys. Res. Lett. 28, 3441–3444.
Shimada, K., Kamoshida, T., Itoh, M., Nishino, S., Carmack, E., McLaughlin, F., Zimmermann, S., Proshutinsky, A., 2006. Pacific Ocean inflow: influence on catastrophic reduction of sea ice cover in the Arctic Ocean. Geophys. Res. Lett., 33.
Souza, A.C., Gardner, W.S., Dunton, K.H., 2014. Rates of nitrification and ammonium dynamics in northeastern Chukchi Sea shelf waters. Deep. Sea Res. Part II: Top. Stud. Oceanogr. 102, 68–76.
Steele, M., Morison, J., Ermold, W., Rigor, I., Ortmeyer, M., Shimada, K., 2004. Circulation of summer Pacific halocline water in the Arctic Ocean. J. Geophys. Res.: Ocean. 109, C02027.
Stroeve, J.C., Kattsov, V., Barrett, A., Serreze, M., Pavlova, T., Holland, M., Meier, W.N., 2012. Trends in Arctic sea ice extent from CMIP5, CMIP3 and observations. Geophys. Res. Lett., 39.
Stroeve, J.C., Maslanik, J., Serreze, M.C., Rigor, I., Meier, W., Fowler, C., 2011. Sea ice response to an extreme negative phase of the Arctic Oscillation during winter 2009/2010, Geophys. Res. Lett. p. 38.
Sylvan, J.B., Dortch, Q., Nelson, D.M., Maier Brown, A.F., Morrison, W., Ammerman, J. W., 2006. Phosphorus limits phytoplankton growth on the Louisiana shelf during the period of hypoxia formation. Environ. Sci. Technol. 40, 7548–7553.
Torres-Valdés, S., Tsubouchi, T., Bacon, S., Naveira-Garabato, A.C., Sanders, R., McLaughlin, F.A., Petrie, B., Kattner, G., Azetsu-Scott, K., Whitledge, T.E., 2013. Export of nutrients from the Arctic Ocean. J. Geophys. Res.: Ocean. 118, 1625–1644.
Tyrrell, T., 1999. The relative influences of nitrogen and phosphorus on oceanic primary production. Nature 400, 525–531.
von Appen, W.-J., Pickart, R.S., 2012. Two configurations of the western Arctic shelfbreak current in summer. J. Phys. Ocean. 42, 329–351.
Walsh, J., McRoy, C., Coachman, L., Goering, J., Nihoul, J., Whitledge, T., Blackburn, T., Parker, P., Wirick, C., Shuert, P., 1989. Carbon and nitrogen cycling within the Bering/Chukchi Seas: source regions for organic matter effecting AOU demands of the Arctic Ocean. Progress Oceanogr. 22, 277–359.
Wang, J., Ikeda, M., 2000. Arctic oscillation and Arctic sea-ice oscillation. Geophys. Res. Lett. 27, 1287–1290.
Wang, J., Zhang, J., Watanabe, E., Ikeda, M., Mizobata, K., Walsh, J.E., Bai, X., Wu, B., 2009. Is the Dipole Anomaly a major driver to record lows in Arctic summer sea ice extent? Geophys. Res. Lett., 36.
Wang, M., Overland, J.E., 2009. A sea ice free summer Arctic within 30 years? Geophys. Res. Lett., 36.
Weber, T.S., Deutsch, C., 2010. Ocean nutrient ratios governed by plankton biogeography. Nature 467, 550–554.
Weingartner, T., Aagaard, K., Woodgate, R., Danielson, S., Sasaki, Y., Cavalieri, D., 2005. Circulation on the north central Chukchi Sea shelf. Deep. Sea Res. Part II: Top. Stud. Oceanogr. 52, 3150–3174.
Wendler, G., Chen, L., Moore, B., 2014. Recent sea ice increase and temperature decrease in the Bering Sea area, Alaska. Theor. Appl. Climatol. 117, 393–398.
Woodgate, R.A., Aagaard, K., Weingartner, T.J., 2006. Interannual changes in the Bering Strait fluxes of volume, heat and freshwater between 1991 and 2004. Geophys. Res. Lett., 33.
Wu, B., Wang, J., Walsh, J.E., 2006. Dipole anomaly in the winter Arctic atmosphere and its association with sea ice motion. J. Clim. 19, 210–225.
Yamamoto-Kawai, M., Carmack, E., McLaughlin, F., 2006. Nitrogen balance and Arctic throughflow. Nature 443, 43.
Zhang, J.-Z., Guo, L., Fischer, C.J., 2010. Abundance and chemical speciation of phosphorus in sediments of the Mackenzie River Delta, the Chukchi Sea and the Bering Sea: importance of detrital apatite. Aquat. Geochem. 16, 353–371.
Zhang, Y., Wallace, J.M., Iwasaka, N., 1996. Is climate variability over the North Pacific a linear response to ENSO? J. Clim. 9, 1468–1478.

Please cite this article as: Piper, M.M., et al., Dissolved and particulate phosphorus distributions and elemental stoichiometry throughout the Chukchi Sea. Deep-Sea Res. II (2016), http://dx.doi.org/10.1016/j.dsr2.2016.05.009